Supporting Information

Performance of a Small-Scale Haber Process: A Techno-Economic Analysis

Bosong Lin,† Theodore Wiesner,† Mahdi Malmali†*

† Department of Chemical Engineering, 807 Canton Ave, Texas Tech University, Lubbock, Texas 79409, United States

*Corresponding author email address: mahdi.malmali@ttu.edu; Tel.: (806) 834-8706; Fax: (806) 742-3552

Number of pages: 37

Number of figures: 8

Number of tables: 16

Nomenclature

Abbreviations

CW	Cooling water
Q_{ch}	Quench
RFG	Refrigerant
RXN-ABS	Reaction-absorption
RXN-CON	Reaction-condensation

Roman symbols

a_k	Gas activity
A_k	Coefficient A of component k
b	Isotherm coefficient
B_k	Coefficient B of component k
c_k	Molar concentration of species k in the bulk gas phase [mol/m^3]
C_k	Coefficient C of component k
D_b	Absorber diameter [m]
$D_{m,k}$	Molecular diffusion coefficient of component k [m^2/s]
$D_{kn,k}$	Knudsen diffusion coefficient [m^2/s]
$E_{z,k}$	Axial dispersion mass transfer coefficient of component k [m^2/s]
F_i	Inlet flow rate [kmol/h]
$J_{abs,K}$	Mass transfer rate due to absorption of component k [mol/m^3 s]
k_2	Reverse reaction coefficient
$k_{f,k}$	Film resistance coefficient [m/s]
K_3	Adsorption equilibrium constant
K_a	Equilibrium constant
K_{pk}	Macro diffusion coefficient [m^2/s]
L	Reactor bed length [m]
M_k	Molecular weight of component k [kg/mol]
MTC_k	LDF rate constant of component k [1/s]
P	Reaction pressure [bar]

r_p	Particle diameter [m]
r_{Pore}	Pore radius [m]
R	Gas constant [J/K mol]
R_{NH_3}	Rate of NH_3 production [kmol/m^3 h]
T	Reaction temperature [°C]
v_g	Gas velocity in axial direction [m/s]
V_k	Diffusion volume of component k
w_k	Absorbent capacity of component k [mol/kg]
w_k^*	Equilibrium capacity of component k [mol/kg]
W_{max}	Maximum capacity [mol/kg]
x_k	Mole fraction of component k
X	Conversion
y_{i,NH_3}	Inlet mole fraction of NH_3
y_{o,NH_3}	Outlet mole fraction of NH_3
z	Axial coordinate of the absorber column

Greek symbols

ε_i	Interparticle voidage
ε_p	Intraparticle voidage
ε_{abs}	Total absorber column voidage
ξ	Extent of reaction
μ_g	Gas dynamic viscosity [kg/m s]
τ_p	Tortuosity of the absorbent particle
τ	Tortuosity factor
ρ_g	Gas density [kg/m^3]
ρ_s	Absorbent density [kg/m^3]
ρ_{abs}	Absorber column density [kg/m^3]
ψ	Particle shape factor

Subscripts and superscripts

abs	Absorber column

g	Gas
i	Interparticle
k	Component k
p	Particle
$pore$	Absorbent partible pore
max	Maximum

1 Simulation

1.1 Ammonia Synthesis Kinetics

To model the synthesis process, ammonia synthesis kinetics described by Nielsen et al. is adopted as shown in Table S1:[1]

Table S1. *Ammonia synthesis kinetics embedded in the reactor of RXN-CON and RXN-ABS.*

Description	Equation	No.	Reference
Rate of NH_3 production	$R_{NH_3} = \left[\frac{k_2\left(a_N K_a^2 - \frac{a_A^2}{a_H^3}\right)}{\left(1 + K_3\frac{a_A}{a_H^\omega}\right)^{2\alpha}}\right]\frac{kgmole}{m^3 hr}$	(S1)	[1]
Equilibrium constant	$log_{10}K_a = -2.691122log_{10}(T) - 5.519265\times10^{-5}T + 1.848863\times10^{-7}T^2 + \frac{2001.6}{T} + 2.6899$	(S2)	[2]
Reaction rate constant	$k_2 = 3.945\times10^{10}\exp\left(-\frac{5622}{T}\right)$	(S3)	[1]
Adsorption equilibrium constant	$K_3 = 2.94\times10^{-4}\exp\left(\frac{12104}{T}\right)$	(S4)	[1]
Gas model	*RKS-BM*	(S5)	[3]
Gas activity	$a_k = x_k P\exp\left[\frac{P}{RT}\left(B_k - \frac{A_k}{RT} - \frac{C_k}{T^3} + \left(A_k^{0.5} - \sum x_k A_k^{0.5}\right)^2\right)\right]$	(S6)	[1]

The values of A_k, B_k, and C_k can be found in Table S2[1]. The reaction kinetics are implemented by a user Fortran subroutine. ω = 1.523 and α = 0.654 are used. Note that R = 0.0826 L·atm·K^{-1}·mol^{-1}, gas constant; P, the pressure in atm; T, the temperature in K.

Table S2. *Values for A, B, C for evaluating the activities for synthesis kinetics*

Component, i	A_k	B_k	C_k
H_2	1.975×10^{-1}	2.096×10^{-2}	5.04×10^{2}
N_2	1.3445	5.046×10^{-2}	4.20×10^{4}
NH_3	2.393	3.415×10^{-2}	4.77×10^{6}

As displayed in Figure S1, the equilibrium conversion was calculated based on Nielsen's kinetics above-mentioned, which is a function of temperature and pressure.

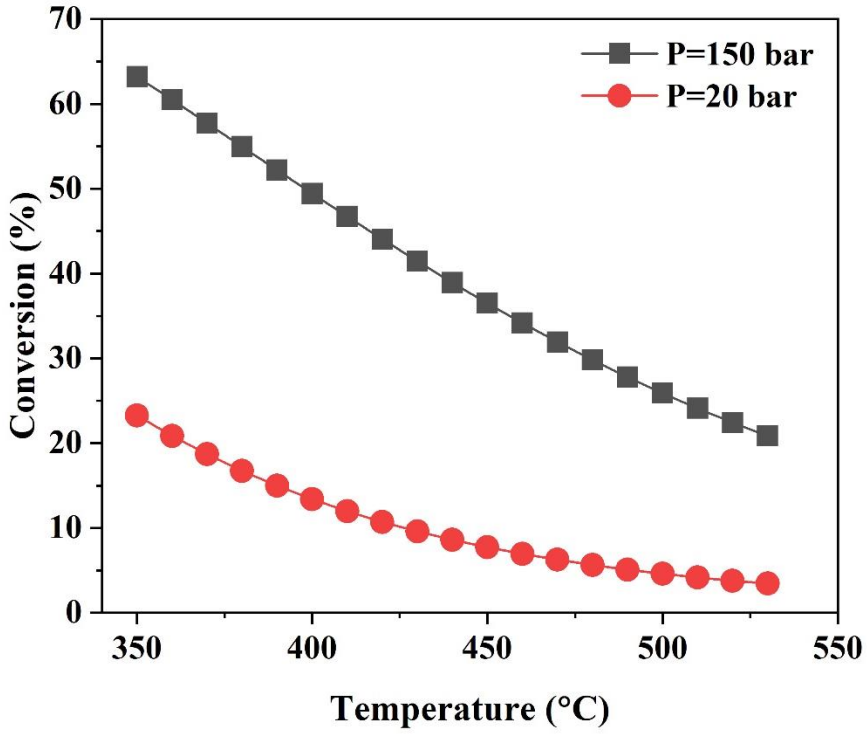

Figure S1. *Equilibrium conversion vs temperature. (RXN-CON at P=150 bar, RXN-ABS at 20 bar)*

1.2 Process Design and Simulation

Table S3*. Design specifications for RXN-CON and RXN-ABS processes*

System/Component	Unit	RXN-CON (110-150 bar)	RXN-ABS (20-35 bar)
Converter R-101			
Bed 1	m	0.5 (D), 0.5 (L)	0.5 (D), 1 (L)
Bed 2	m	0.5 (D), 0.7 (L)	0.5 (D), 2 (L)
Bed 3	m	0.5 (D), 1 (L)	0.5 (D), 3 (L)
Total length	m	2.2	6
Mainstream fraction	%	0.6	0.6
Quench fraction	%	0.4	0.4
Inlet temperature	°C	350	350
Catalyst density	kg/m3	2200	2200
Void fraction	%	05	0.5
Turbomachinery (C-101, C-102)			
Isentropic efficiencies	%	70	70
Mechanical efficiencies	%	95	95
Cooling Water			
Inlet temperature	°C	20	20
Outlet temperature	°C	35	35
Pressure	bar	5	5
Pump efficiency	%	85	85
Refrigerant			
Temperature	°C	-50	/
Absorbers			
Absorption	°C	/	150
Desorption	°C	/	300
No of absorber columns	/	/	3

Results of ammonia mole fraction along the bed (see Figure S2) were obtained from simulation. In the RXN-CON process (Figure S2a), the gas mixture that enters the converter contains 1.5 mol% of ammonia because the phase-changing condensation is not capable of separating 100% of ammonia. On the other hand, the ammonia mole fraction in the gas mixture entering the converter in the RXN-ABS process (Figure S2b) is close to zero because the absorber column almost completely removes the ammonia from the recycle gas until it breaks through. As reactants enter the three-bed ammonia converter, ammonia mole fraction increases due to the formation of ammonia. At the end of the first and second beds, ammonia mole fraction decreases because the streams leaving the bed were diluted by the quench streams. The highest ammonia mole fraction in RXN-CON is about 2.5 times higher than that of RXN-ABS because of higher operating pressure in RXN-CON. Then these results as displayed in Figure S2 were converted into the conversion of nitrogen.

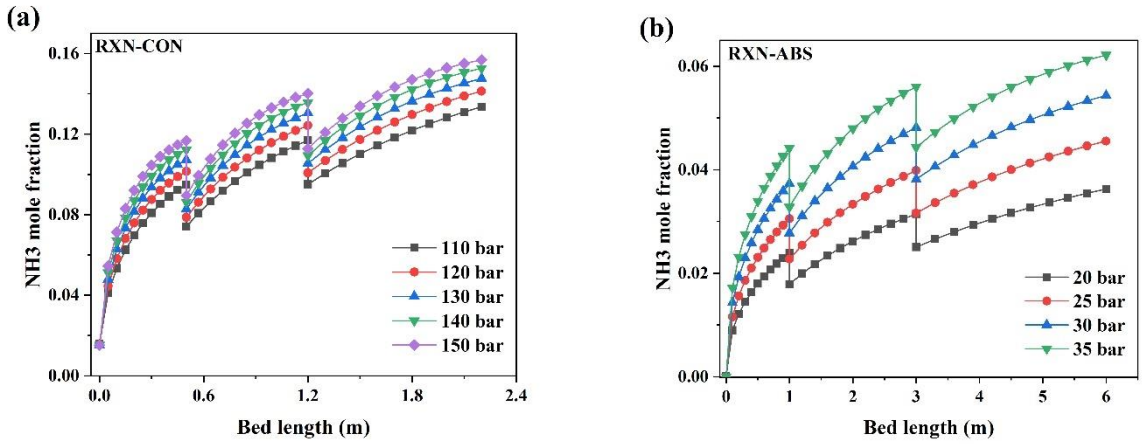

***Figure S2**. Ammonia mole fraction along the bed in RXN-CON (a) and RXN-ABS (b).*

***Table S4.** Converting ammonia mole fraction to conversion based on simulation results*

Description	**Equation**	**No.**
Outlet mole fraction of NH_3	$y_{o,NH_3} = \frac{F_i y_{i,NH_3} + 2\xi}{F_i - 2\xi}$	(S7)
Extent of reaction	$\xi = \frac{F_i\left(y_{o,NH_3} - y_{i,NH_3}\right)}{2\left(1 + y_{o,NH_3}\right)}$	(S8)
Conversion	$X = \frac{\xi}{F_i y_{i,N_2}} = \frac{2\left(y_{o,NH_3} - y_{i,NH_3}\right)}{\left(1 + y_{o,NH_3}\right)\left(1 - y_{o,NH_3}\right)}$	(S9)

Table S5. *Stream table for the operating condition for the RXN-CON process.*

Stream	**1**	**2**	**3**	**4**	**5**	**6**	**7**
Temperature (°C)	25	25	24.7194	531.492	105.084	109.307	127.682
Pressure (bar)	10	10	9.5	150	146	150	149.5
Molar vapor fraction	1	1	1	1	1	1	1
Mole flows (kmol/h)	214.298	71.3942	285.693	285.693	1172.93	1172.93	1172.92
H_2 (kmol/h)	214.298	0	214.298	214.298	892.098	892.098	892.084
N_2 (kmol/h)	0	71.3942	71.3942	71.3942	267.606	267.606	267.617
NH_3 (kmol/h)	0	0	0	0	13.2228	13.2228	13.2225
Water (kmol/h)	0	0	0	0	0	0	0
Mole fractions							
H_2	1	0	0.750101	0.750101	0.760574	0.760574	0.760564
N_2	0	1	0.249899	0.249899	0.228152	0.228152	0.228163
NH_3	0	0	0	0	0.0112734	0.0112734	0.0112731
Water	0	0	0	0	0	0	0
Mass flows (kg/h)	432	2000	2432	2432	9520.13	9520.13	9520.42
H_2 (kg/h)	432	0	432	432	1798.36	1798.36	1798.33
N_2 (kg/h)	0	2000	2000	2000	7496.58	7496.58	7496.9
NH_3 (kg/h)	0	0	0	0	225.192	225.192	225.187
Water (kg/h)	0	0	0	0	0	0	0
Mass fractions							
H_2	1	0	0.177632	0.177632	0.188901	0.188901	0.188892
N_2	0	1	0.822368	0.822368	0.787445	0.787445	0.787455
NH_3	0	0	0	0	0.0236543	0.0236543	0.023653
Water	0	0	0	0	0	0	0

Continued

Stream	**8 (Q_{ch}-1)**	**9 (Q_{ch}-2)**	**9 (Q_{ch}-3)**	**10**	**11**	**12**	**13**
Temperature (°C)	127.682	127.682	127.682	350	479.185	340.653	321.292
Pressure (bar)	149.5	149.5	149.5	149	147.5	147	146.5
Molar vapor fraction	1	1	1	1	1	1	1
Mole flows (kmol/h)	703.754	234.585	234.585	703.752	1030.32	1030.32	1030.32
H_2 (kmol/h)	535.25	178.417	178.417	535.248	678.175	678.175	678.175
N_2 (kmol/h)	160.57	53.5235	53.5235	160.57	196.315	196.315	196.315
NH_3 (kmol/h)	7.9335	2.6445	2.6445	7.93329	155.827	155.827	155.827
Water (kmol/h)	0	0	0	0	0	0	0
Mole fractions							
H_2	0.760564	0.760564	0.760564	0.760564	0.65822	0.65822	0.65822
N_2	0.228163	0.228163	0.228163	0.228163	0.190538	0.190538	0.190538
NH_3	0.0112731	0.0112731	0.0112731	0.0112729	0.151242	0.151242	0.151242
Water	0	0	0	0	0	0	0
Mass flows (kg/h)	5712.25	1904.08	1904.08	5712.23	9520.4	9520.4	9520.4
H_2 (kg/h)	1079	359.667	359.667	1079	1367.12	1367.12	1367.12
N_2 (kg/h)	4498.14	1499.38	1499.38	4498.13	5499.46	5499.46	5499.46
NH_3 (kg/h)	135.112	45.0373	45.0373	135.108	2653.82	2653.82	2653.82
Water (kg/h)	0	0	0	0	0	0	0
Mass fractions							
H_2	0.188892	0.188892	0.188892	0.188892	0.143599	0.143599	0.143599
N_2	0.787455	0.787455	0.787455	0.787455	0.57765	0.57765	0.57765
NH_3	0.023653	0.023653	0.023653	0.0236525	0.278751	0.278751	0.278751
Water	0	0	0	0	0	0	0

Continued

Stream	**14**	**15**	**16**	**17**	**CW-In**	**CW-Out**	**RFG-In**	**RFG-Out**
Temperature (°C)	40	40	-29.121	-29.121	20	30.896	-50	-32.6067
Pressure (bar)	146	146	146	146	5	4.5	1.01325	1.01325
Molar vapor fraction	1	1	1	0	0	0	0	1
Mole flows (kmol/h)	1044.84	1030.32	887.24	143.076	9991.52	9991.52	206.392	206.392
H_2 (kmol/h)	669.734	678.175	677.814	0.361061	0	0	0	0
N_2 (kmol/h)	214.347	196.315	196.204	0.111256	0	0	0	0
NH_3 (kmol/h)	160.756	155.827	13.2228	142.604	0	0	206.392	206.392
Water (kmol/h)	0	0	0	0	9991.52	9991.52	0	0
Mole fractions								
H_2	0.640994	0.65822	0.763958	0.00252355	0	0	0	0
N_2	0.205149	0.190538	0.221139	0.000777601	0	0	0	0
NH_3	0.153858	0.151242	0.0149032	0.996699	0	0	1	1
Water	0	0	0	0	1	1	0	0
Mass flows (kg/h)	10092.5	9520.4	7087.93	2432.47	180000	180000	3514.97	3514.97
H_2 (kg/h)	1350.1	1367.12	1366.39	0.727855	0	0	0	0
N_2 (kg/h)	6004.6	5499.46	5496.34	3.11668	0	0	0	0
NH_3 (kg/h)	2737.77	2653.82	225.191	2428.63	0	0	3514.97	3514.97
Water (kg/h)	0	0	0	0	180000	180000	0	0
Mass fractions								
H_2	0.133773	0.143599	0.192777	0.000299224	0	0	0	0
N_2	0.594958	0.57765	0.775452	0.00128128	0	0	0	0
NH_3	0.271268	0.278751	0.0317711	0.998419	0	0	1	1
Water	0	0	0	0	1	1	0	0

Table S6. *Stream table for the operating condition for the RXN-ABS process.*

Stream	**1**	**2**	**3**	**4**	**5**	**6**	**7**	**8 (Q_{ch}-1)**
Temperature (°C)	25	25	24.7194	125.914	148.317	166.638	290	290
Pressure (bar)	10	10	9.5	20	18	20	19.9	19.9
Molar vapor fraction	1	1	1	1	1	1	1	1
Mole flows (kmol/h)	214.298	71.3942	285.693	285.693	4076.29	4076.29	4076.29	2445.78
H_2 (kmol/h)	214.298	0	214.298	214.298	3057.25	3057.25	3057.25	1834.35
N_2 (kmol/h)	0	71.3942	71.3942	71.3942	1019.04	1019.04	1019.04	611.427
NH_3 (kmol/h)	0	0	0	0	0	0	0	0
Water (kmol/h)	0	0	0	0	0	0	0	0
Mole fractions								
H_2	1	0	0.750101	0.750101	0.750007	0.750007	0.750007	0.750007
N_2	0	1	0.249899	0.249899	0.249993	0.249993	0.249993	0.249993
NH_3	0	0	0	0	0	0	0	0
Water	0	0	0	0	0	0	0	0
Mass flows (kg/h)	432	2000	2432	2432	34710	34710	34710	20826
H_2 (kg/h)	432	0	432	432	6163.05	6163.05	6163.05	3697.83
N_2 (kg/h)	0	2000	2000	2000	28547	28547	28547	17128.2
NH_3 (kg/h)	0	0	0	0	0	0	0	0
Water (kg/h)	0	0	0	0	0	0	0	0
Mass fractions								
H_2	1	0	0.177632	0.177632	0.177558	0.177558	0.177558	0.177558
N_2	0	1	0.822368	0.822368	0.822442	0.822442	0.822442	0.822442
NH_3	0	0	0	0	0	0	0	0
Water	0	0	0	0	0	0	0	0

Continued

Stream	**9 (Q_{ch}-2)**	**9 (Q_{ch}-3)**	**10**	**11**	**12**	**13**	**14**	**15**
Temperature (°C)	290	290	350	387.847	351.419	343.459	218.108	150
Pressure (bar)	19.9	19.9	19.8	18.3	18.2	18.1	18	18
Molar vapor fraction	1	1	1	1	1	1	1	1
Mole flows (kmol/h)	815.259	815.259	2445.78	3933.68	3933.68	3933.68	3933.33	3933.33
H_2 (kmol/h)	611.45	611.45	1834.35	2843.33	2843.33	2843.33	2843.07	2843.07
N_2 (kmol/h)	203.809	203.809	611.427	947.737	947.737	947.737	947.652	947.652
NH_3 (kmol/h)	0	0	0	142.614	142.614	142.614	142.605	142.605
Water (kmol/h)	0	0	0	0	0	0	0	0
Mole fractions								
H_2	0.750007	0.750007	0.750007	0.722816	0.722816	0.722816	0.722816	0.722816
N_2	0.249993	0.249993	0.249993	0.240929	0.240929	0.240929	0.240929	0.240929
NH_3	0	0	0	0.036255	0.036255	0.036255	0.036256	0.036256
Water	0	0	0	0	0	0	0	0
Mass flows (kg/h)	6942	6942	20826	34710	34710	34710	34707	34707
H_2 (kg/h)	1232.61	1232.61	3697.83	5731.81	5731.81	5731.81	5731.29	5731.29
N_2 (kg/h)	5709.39	5709.39	17128.2	26549.4	26549.4	26549.4	26547	26547
NH_3 (kg/h)	0	0	0	2428.79	2428.79	2428.79	2428.64	2428.64
Water (kg/h)	0	0	0	0	0	0	0	0
Mass fractions								
H_2	0.177558	0.177558	0.177558	0.165134	0.165134	0.165134	0.165134	0.165134
N_2	0.822442	0.822442	0.822442	0.764892	0.764892	0.764892	0.764891	0.764891
NH_3	0	0	0	0.069974	0.069974	0.069974	0.069976	0.069976
Water	0	0	0	0	0	0	0	0

Continued

Stream	**16**	**Product**	**CW2-In**	**CW2-Out**	**CW1-In**	**CW1-Out**
Temperature (°C)	150	36	20	35.0005	20	35
Pressure (bar)	18	15.4	1.01325	1.01325	1.01325	0.91325
Molar vapor fraction	1	0.029844	0	0	0	0
Mole flows (kmol/h)	3790.6	142.979	3346.86	3346.86	6142.62	6142.62
H_2 (kmol/h)	2842.95	0.280076	0	0	0	0
N_2 (kmol/h)	947.65	0.094073	0	0	0	0
NH_3 (kmol/h)	0	142.605	0	0	0	0
Water (kmol/h)	0	0	3346.86	3346.86	6142.62	6142.62
Mole fractions						
H_2	0.75	0.001959	0	0	0	0
N_2	0.25	0.000658	0	0	0	0
NH_3	0	0.997383	0	0	0	0
Water	0	0	1	1	1	1
Mass flows (kg/h)	32278	2431.84	60294.6	60294.6	110661	110661
H_2 (kg/h)	5731.05	0.5646	0	0	0	0
N_2 (kg/h)	26547	2.6353	0	0	0	0
NH_3 (kg/h)	0	2428.64	0	0	0	0
Water (kg/h)	0	0	60294.6	60294.6	110661	110661
Mass fractions						
H_2	0.177553	0.000232	0	0	0	0
N_2	0.822447	0.001084	0	0	0	0
NH_3	0	0.998684	0	0	0	0
Water	0	0	1	1	1	1

Note: the stream table was generated from the steady state model, with the absorber column desorbing at 300 C. The integration between the absorber and reactor is not considered in the calculation of the temperature for S12 and S13.

1.3 Dynamic Modeling of an Absorption Column

Table S7. *Summary of the equations of the dynamic absorption Column model.*[4]

Description	Equation	No.
Mass balance for the gas phase	$-\varepsilon_i E_{zk}\frac{\partial^2 c_k}{\partial z^2}+\frac{\partial(v_g c_k)}{\partial z}+\varepsilon_B\frac{\partial c_k}{\partial t}+(1-\varepsilon_i)J_{abs}=0$	(S10)
Mass transfer due to absorption	$J_{abs}=\rho_s\frac{\partial w_k}{\partial t}$	(S11)
Kinetic model Linear driving force	$\frac{\partial w_k}{\partial t}=MTC_k(w_k^*-w_k)$	(S12)
Equilibrium capacity	$w_k^*=w_{max}\frac{bp_k}{1+bp_k}$	(S13)
Gas model	RKS-BM	(S14)
Momentum balance: Ergun equation	$\frac{dp}{dz}=\frac{1.5\times10^{-3}(1-\varepsilon_i)^2\mu v_g}{(2r_p\psi)^2\varepsilon_i{}^3}+\frac{1.75\times10^{-5}M\rho_g(1-\varepsilon_i)}{2r_p\psi\varepsilon_i{}^3}{v_g}^2$	(S15)
Dispersion coefficient	$E_{zk}=0.73D_{mk}+\frac{v_g r_p}{\varepsilon_i\left(1+9.49\frac{\varepsilon_i D_{mk}}{2v_g r_p}\right)}$	(S16)
Effective molecular diffusion coefficient	$D_{mk}=\frac{10^{-3}T^{1.73}\left(\frac{1}{M_k}+\frac{1}{M_m}\right)^{1/2}}{P[(\sum V_k)^{1/3}+(\sum V_m)^{1/3}]^2}$	(S17)
Effective mass transfer coefficient	$\frac{1}{MTC_k}=\frac{r_p}{2k_{fk}}+\frac{r_p^2}{15\varepsilon_p K_{pk}}$	(S18)
Film resistance coefficient	$k_{fk}=Sh_k\frac{D_{mk}}{2r_p}$	(S19)
Macro diffusion coefficient	$\frac{1}{K_{pk}}=\tau\left(\frac{1}{D_{kn,k}}+\frac{1}{D_{mk}}\right)$	(S20)
Knudsen diffusion coefficient	$D_{kn,k}=97r_{Pore}\left(\frac{T}{M_k}\right)^{0.5}$	(S21)
Total column voidage	$\varepsilon_B=\varepsilon_i+(1-\varepsilon_i)\varepsilon_p$	(S22)

Reynolds number	$Re = \frac{v_g d_p \rho_g}{\mu_g}$	(S23)
Schmidt number	$Sc_k = \frac{\mu_g D_m}{\rho_g}$	(S24)
Sherwood number	$Sh_k = 2 + 1.1 Sc^{1/3} Re^{0.6}$	(S25)
Tortuosity factor	$\tau = \tau_p + 1.5(1 - \varepsilon_p)$	(S26)
Initial conditions	$c_{k,i} = 0; w_{k,i} = 0;\ i = 0, 1, 2, \cdots$	(S27)
Boundary conditions	$c_{k,0} = c_{k,feed};\ v_g = v_{g,feed};\ P = P_{feed}$	(S28)

The mathematical model is solved by the finite difference method with initial conditions and boundary conditions. The model is then validated by experimental data of breakthrough time for the selected absorbent.

1.4 Absorber Specifications

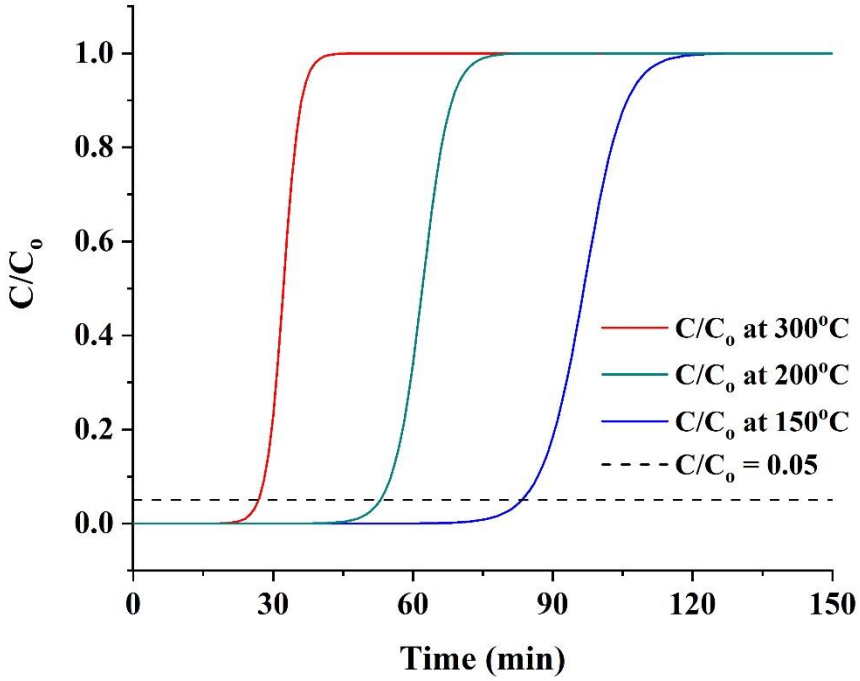

Figure S3. *Breakthrough time of ammonia absorption with MgBr2-Si at 100 °C, 200 °C, and 300 °C. Conditions used in simulation are consistent with those in experiments*[5]*. The breakthrough time threshold is 5% of the feed concentration.*

Table S8. *Experimental results vs simulation results (Breakthrough time of ammonia absorption with MgBr2-Si at 100 °C, 200 °C, and 300 °C)*

Temperature [°C]	**Breakthrough Time [min]**		
	Experimental Results	**Simulation Results**	**Error [%]**
150	81	82.1	1.4
200	52	52.4	0.8
300	28	27.0	3.6

The ammonia capacity of the selected absorbent, $MgBr_2$-Si, at different temperatures (423 K, 473 K, and 573 K):[5]

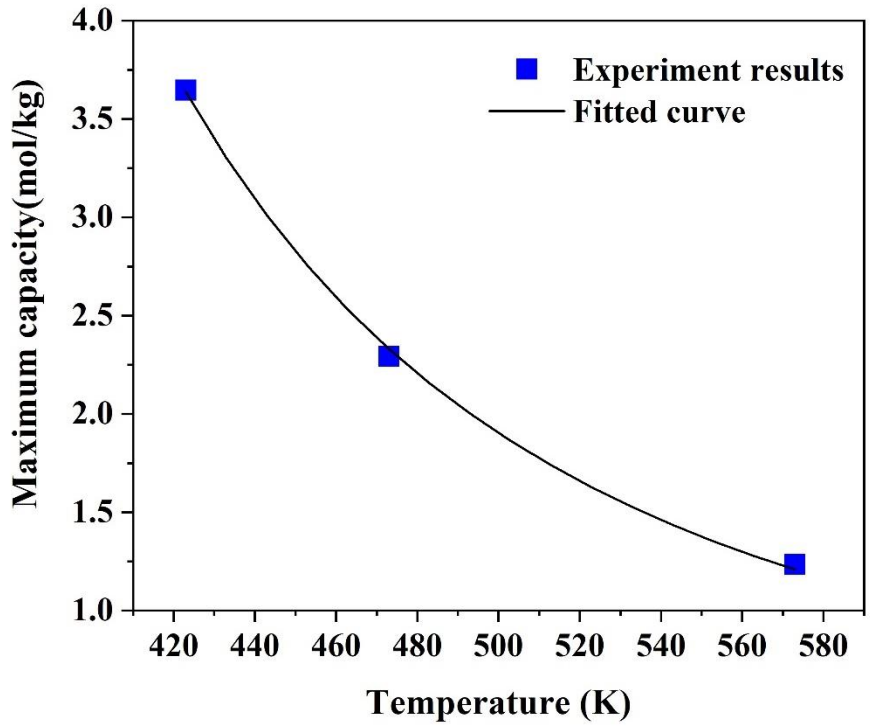

***Figure S4**. Ammonia capacity of $MgBr_2$-Si at 100 °C, 200 °C, and 300 °C (experiments retrieved from[5])*

The expression for the fitted curve:

$$W_{max} = 0.05411\exp\left(\frac{1780}{T(°C) + 273.15}\right) \quad \text{(S29)}$$

Lab-scale result can provide us an initial guessing of the absorber size, specifically, the size can be simply calculated based on the hourly ammonia production and the coordination number of the ammine complex of $MgBr_2$-NH_3. Given that 2428.8 kg/hr. of ammonia is synthesized in the proposed ammonia plant, the amount of ammonia absorbed by $MgBr_2$ for 30 minutes in an absorber column during a PSA/TSA cycle can be obtained as follows:

$$2{,}428.8\frac{kg}{hr}\cdot 1000\cdot\frac{kmol}{17.031kg}\cdot\frac{1}{2}=71{,}436.32\ mol$$

Given that the complex $Mg(NH_3)_{1.5}Br_2$ is formed during absorption, the amount of $MgBr_2$ in one absorber bed is

$$71436.32\ \frac{mol}{1.5}\cdot\frac{kmol}{1000\ mol}\cdot\frac{184\ kg}{kmol}=8768\ kg$$

With the density of 3720 kg/m^3 of $MgBr_2$, bed voidage of 0.32, and particle voidage of 0.4, the volume of the absorber can be calculated as

$$V=8768\ \ kg/\ 3720\frac{kg}{\mathrm{m}^3}/\frac{1}{(1-0.32)(1-0.4)}=5.74\ m^3$$

If the length-to-diameter ratio is 2.5, back-calculate the length and diameter with the formula below, thus, D = 1.43 m and L = 3.58 m.

$$V=\frac{LD^2\pi}{4}=\frac{2.5D^3\pi}{4}$$

When the initial size was used in our dynamic modeling of an absorber column, it shows that breakthrough happens at 11 mins, shown as a black line in Figure S5, which indicates the discrepancy between the lab scale and the proposed scale. The space velocity from the simulation is also not close to that of the lab scale. The volumetric flow of the stream entering the absorber was 11301 m^3/h while the flow rate in the las scale was 0.005578 m^3/h with the bed size of 1.92×10^{-5} m^3. The resulted space velocity of the proposed design and the lab scale was 1968/h and 289/h, respectively. Therefore, it is important to note that the coordination number of the complex ammine obtained in the lab scale could not be achieved in the proposed design.

The final size of the absorber column was tuned to achieve the absorption time of 30 mins. A red line in Figure S5 denotes the outlet composition of the absorber in the final design (4.70 m

length, 1.88 m diameter, with volume of 13.87 m^3), indicating that breakthrough will happen at 30 mins. Thus, this size was used in the design.

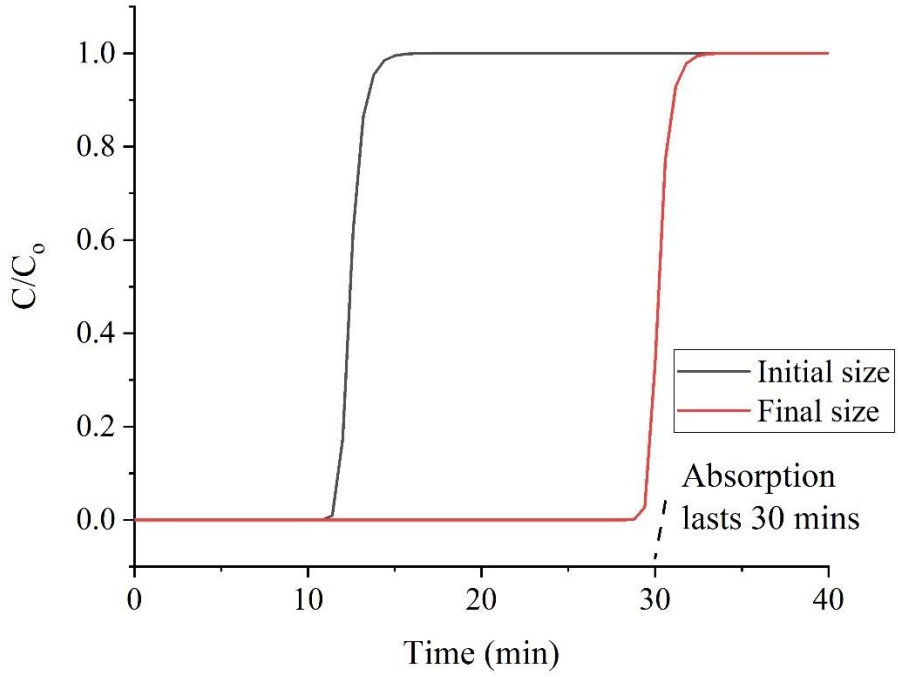

***Figure S5**. Breakthrough time for initial and final design of the absorber size. NH_3 mole fraction was normalized by the initial composition of NH_3 before entering the absorber. Breakthrough takes places as C/C_o reaches 0.05. The black line represents the initial size (5.74 m^3) inspired from the lab-scale result, showing that breakthrough happens at 11 mins. The red line denotes the outlet composition of the absorber in the final design (13.87 m^3), indicating that breakthrough will happen at 30 mins.*

1.5 RXN-ABS Heat Integration Strategy

To summarize, in the reaction-absorption process (RXN-ABS), the reactor effluent stream will be directed to the absorber that in the desorption mode and at preheating stage (Step 2). Specifically, the absorber is chosen to be a shell-and-tube column, therefore heat of reaction can be recovered as the reactor effluent flows via the shell side of the regenerating column. This stream will be further cooled with cooling water and then directed to the absorber column in the process line (Step 1) for the separation of ammonia. In addition to the sensible heat needed for raising the temperature of absorber column and absorbent, the heat of desorption of ammonia should be also provided. The specific heat capacity of stainless-steel absorber column and absorbent particles is about 0.50 J/(g·°C)[6] and 0.32 J/(g·°C)[7]. Integrating heat from reaction for the regenerating column was carried out via ASPEN Plus, from which we obtain information on the streams in a steady state.

In general, the whole process is exothermic. We assume that reactor and absorber column can be tightly heat integrated, while the heat of reaction released from the ammonia synthesis can be directed to cancel the heat requirements beyond the pinch point (minimum temperature approach of 10°C). For this design, we simply used the water cooling for reducing the temperature of the reactor effluent before the separation and refrigeration and to keep the temperature of the absorber constant during the absorption stage (Step 1). We found that these costs are insignificant and had less than 1% effect on the final LCOA. See the calculation of absorber cooling costs during Step 1 in Section 1.9).

1.6 Capital Costs of RXN-CON and RXN-ABS

Table S9. *Total Capital Costs for RXN-CON at 150 bar and RXN-ABS at 20 bar.*

Subsystem	Capital Investment [$ millions]			
	RXN-CON	**%**	**RXN-ABS**	**%**
Hydrogen production	21.04	62	21.04	67
Nitrogen production	0.68	2	0.68	2
Synthesis loop	12.43	36	10.29	31
Total	34.26	100	32.11	100

Table S10. *K values for estimation of equipment cost used with Eq. (2).*[8]

Equipment	K_1	K_2	K_3	**Capacity, Units**	**Min Size**	**Max Size**
Centrifugal Compressors	2.2897	1.3604	-0.1027	Fluid Power, kW	450	3000
Rotary Compressors	5.0355	-1.8002	0.8253	Fluid Power, kW	18	950
Electric Drives	1.956	1.7142	-0.2282	Shaft Power, kW	75	2600
Floating Head Heat Exchangers	4.8306	-0.8509	0.3187	Area, m^2	10	1000
Reciprocating Pump	3.8696	0.3161	0.1220	Shaft Power, kW	0.1	200
Packed Tower (Reactor/Absorber)	3.4974	0.4485	0.1074	Volume, m^3	0.3	520

Table S11. *Bare module cost factors for the equipment purchased in ammonia synthesis loop in RXN-CON (150 bar)*

Equipment No.	**Equipment Type**	F_{BM}	C_P^0 **($) (2001)**	C_{BM} **($) (2019)**
E-101	Heat Exchanger	7.48	3,730	44,550
E-102	Heat Exchanger	7.43	2,210	26,221
E-103	Heat Exchanger	8.04	18,640	239,284
R-101	Reactor	76.98	2,310	284,020
C-101	Compressor	5.80	321,547	2,978,808
C-102	Compressor	5.80	15,822	146,571
V-101	Vessel	66.51	1,726	183,331
D-101	Drive	1.50	119,790	287,000
D-102	Drive	1.50	23,330	55,895
P-101	Pump	1.85	6,560	19,384
E-104	Heat Exchanger	8.04	19,994	256,669
Refrigeration				
E-201	Heat Exchanger	8.04	21,649	277,922
C-201	Compressor	5.80	163,813	1,517,562
D-201	Drive	1.50	124,216	297,605
P-201	Pump	1.85	3,950	11,672
Total				6,626,494
CEPCI	634 (Oct 2019)	397 (Sep 2001)		

Table S12. *Bare module cost for the equipment purchased in ammonia synthesis loop RXN-CON (150 bar) and RXN-ABS (20 bar).*

Equipment No.	**Equipment Type**	F_{BM}	C_P^0 **(\$) (2001)**	C_{BM} **(\$) (2019)**
E-101	Heat Exchanger	1.74	18,528	51,492
E-102	Heat Exchanger	1.74	24,365	67,716
E-103	Heat Exchanger	1.74	18,540	51,525
R-101	Reactor	36.89	7,045	415,076
C-101	Compressor	5.80	86,619	802,438
C-102	Compressor	5.80	183,990	1,704,488
D-101	Drive	1.50	56,282	134,843
D-102	Drive	1.50	91,283	218,701
P-101	Pump	1.85	2,760	8,156
P-102	Pump	1.85	2,493	7,365
V-101	Absorber Columns	36.61	22,692	2,492,109
Total				5,953,909
CEPCI	634 (Oct 2019)	397 (Sep 2001)		

1.7 Operating Costs of RXN-CON and RXN-ABS

Table S13. *Raw Materials, Utilities, Waste Treatment, and Operating Labor for RXN-CON (150 bar).*

RXN-CON (150 bar)	**Current Price, $/kg**	**Amount Purchased, kg/yr.**	**Annual Cost, $/yr.**
Raw Materials			
Feed Water, kg	0.005	31,764,246	143,383
Iron Catalyst, kg	2.700	6,476	17,486
Total Raw Material Costs, C_{RM}			160,869
Utilities			
Cooling Water, kg	2.58×10^{-5}	10,790,114,112	278,321
Refrigerants, GJ	14.3	103,753	1,487,824
Electric Power, kWh	0.04	193,951,966	7,952,031
Total Annual Utility Cost, C_{UT}			9,718,176
Waste Treatment, C_{WT}	–	–	–
	Total Number of Operators	Operator Base Wages +Benefits, $/yr.	Cost of Operating Labor, $/yr.
Operating Labor, C_{OL}	28	54,080	1,514,240

Table S14. *Raw Materials, Utilities, Waste Treatment, and Operating Labor for RXN-ABS (20 bar).*

RXN-ABS (20 bar)	**Current Price, $/kg**	**Amount Purchased, kg/yr.**	**Annual Cost, $/yr.**
Raw Materials			
Feed Water, kg	0.005	31,764,246	143,383
Iron Catalyst, kg	2.700	17,663	47,689
Absorbent, kg	1	174,248	174,248
Total Raw Material Costs, C_{RM}			365,320
Utilities			
Cooling Water, kg	2.58×10^{-5}	14,700,096,000	379,176
Electric Power, kWh	0.04	187,221,604	7,676,086
Total Annual Utility Cost, C_{UT}			8,055,261
Waste Treatment, C_{WT}	–	–	–
	Total Number of Operators	Operator Base Wages +Benefits, $/yr.	Cost of Operating Labor, $/yr.
Operating Labor, C_{OL}	28	54,080	1,514,240

1.8 Wind Generation Capacity

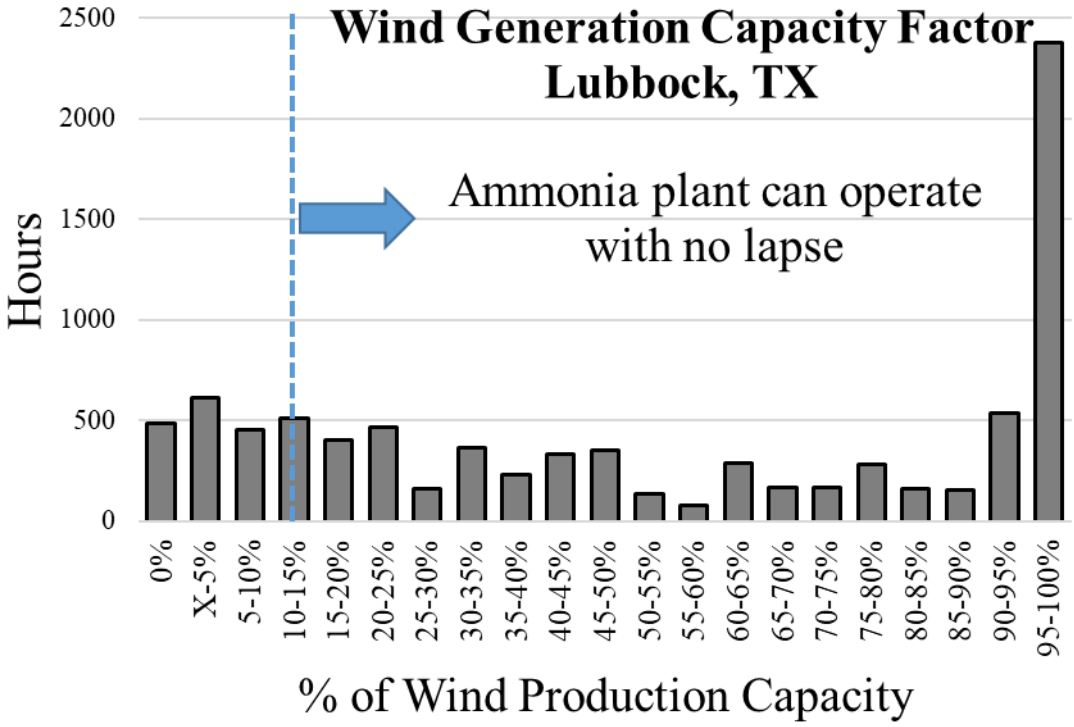

Figure S6. *Wind generation in TTU's GLEAMM microgrid facility, located at Lubbock, TX operating at a stream factor of 0.94 (total working hours of 8760 hours).*

1.9 Power Requirement for Cooling in Absorption Step

We evaluated the possible heat released during ammonia uptake. Malmali et al.[5] reported that the coordination number of $MgBr_2$-NH_3 is 1.5 mol_{NH3}/mol_{salt} at 150 °C. If the complex $Mg(NH_3)_{1.5}Br_2$ is formed during absorption, the amount of heat released due to absorption can be obtained by multiplying the ammonia produced by the heat of absorption as follows:

$$Q = \Delta H_{abs} \cdot P_{NH_3} \cdot MW_{NH_3}$$

$$= (90.80 + 84.10 * 0.5)\frac{kJ}{mol} \cdot 2428\frac{kg}{hr} \cdot 17.031\frac{kg}{kmol} = 5{,}493{,}516\frac{kJ}{hr}$$

We assumed that the generated heat can be removed by cooling water, without design a heat integration with other processes. The amount of cooling water can be calculated by

$$M_{water} = \frac{Q}{C_p \cdot \Delta T}$$

which results in $M_{water} = 65{,}680\frac{kg}{hr}$ ($C_p = 4182\frac{J}{kg°C}, \Delta T_{difference} = 20$).

The pumping power is then obtained by heuristics as follows:

$$P_{pump} = \frac{1.67 \cdot M_{water}\ (\frac{m^3}{\min}) \cdot \Delta P}{\eta_{pump}}$$

If the reciprocating pump is assumed to have a pressure drop of 2 bar with a pump efficiency of 85%, then the total pumping power is 4.30 kW, approximately 0.017 kWh/kg NH_3, which is about 0.18% of total energy consumption. Therefore, it is reasonable to assume that the power requirement for cooling can be negligible.

The utility cost resulted from this amount of cooling water can be calculated by multiplying the amount of cooling water during by its costs – with an annual stream factor of 0.94,

$$C_{ut,water} = M_{water} \cdot 2.58 \times 10^{-5}\frac{\$}{kg} \cdot 365\ days \cdot 24\ hr \cdot 0.94 = \$14{,}000/year$$

The additional utility cost for cooling, $C_{ut,water}$ results in increasing the operating cost by \$17,220/year using Eq. 6 in the manuscript, which results in an increase on LCOA by \$1.41 MT

of NH_3. Therefore, it is reasonable to assume that cost of cooling water for the absorption step has negligible impact on the result.

Overall, heat management of such process is a multi-objective optimization problem and needs its own dedicated study, which is beyond the scope of this work.

1.10 Improving Economics by Selling Oxygen

Oxygen is produced during nitrogen production via PSA and hydrogen production via electrolysis of water. Also, we assume that PSA can produce high-purity oxygen with additional facilities. PSA produces 607.6 kg/hr. O_2, given that nitrogen mass flow is 2000 kg/hr., the weight ratio of 1:3.29, while electrolysis of water produces 3428.8 kg/hr. O_2, given that hydrogen mass flow is 428.6 kg/hr. and the weight ratio of 1:8. Therefore the total amount of oxygen generated is 4036.4 kg/hr. O_2 will be stored in medical E oxygen tanks which have service pressure of 2,015 psi with a volume of 682 L. The cost of an empty medical tank is $64.60/cylinder.[9] After packaging the oxygen in the cylinder, O_2 can be sold for $125/tank.[10]

The volume of the amount of oxygen produced can be calculated using the ideal gas law:

$$V = \frac{\dot{m}RT}{MP} = \frac{4036.4 \cdot 1000\frac{g}{hr} \cdot 0.0821\frac{L \cdot atm}{mol \cdot K} \cdot 298.15\ K}{32\frac{g}{mol} \cdot 137.11\ atm} = 22.520\frac{L}{hr}$$

The number of tanks needed per hour can be calculated by

$$N_{\frac{tanks}{hr}} = \frac{V}{Volume/tank} = \frac{22{,}520\frac{L}{hr}}{682\frac{L}{tank}} = 33\frac{tanks}{hr}$$

Cost of tanks per year can then be found by:

$$Cost_{tank} = 33\frac{tanks}{hr} \cdot 64.60\frac{USD}{tank} \cdot 24\frac{hr}{day} \cdot 365\ \frac{days}{year} \cdot 0.94 = 17{,}619{,}410\ \frac{USD}{year}$$

The resulting income from selling the oxygen can be estimated by:

$$Cost_{O2} = 33\frac{tanks}{hr} \cdot 125\frac{USD}{tank} \cdot 24\frac{hr}{day} \cdot 365\ \frac{days}{year} \cdot 0.94 = 33{,}988{,}061\ \frac{USD}{year}$$

Then the net profit from selling the oxygen is

$$Cost_{O2} - Cost_{tank} = 33{,}988{,}061\ \frac{USD}{year} - 17{,}619{,}410\ \frac{USD}{year} = 16{,}368{,}650\frac{USD}{year}$$

1.11 Cash Flow (RXN-ABS) – Selling Oxygen

This 20,000 MT/year ammonia plant can be profitable if selling oxygen produced from PSA and electrolysis of water. As in Table S15, a cash flow table was constructed assuming a 20-year project life span with an additional 2 years added before the project begins for investment and plant construction. Total capital investment, annual revenue (from selling oxygen and ammonia), annual operating cost, after-tax Rate of return, cost of capital, and NPV at cost of capital are summarized. In Figure S7, non-discounted cash flow diagram show that the plant can profit after 5 years.

Table S15. *Executive Summary (RXN-ABS, 20 bar)*

Executive Summary	
Total Capital Investment, TCI	$31.61 million
Selling Price of Ammonia	$598/MT of ammonia[11]
Annual Revenue: Ammonia	$11.96 million
Annual Revenue: Oxygen	$16.37 million
Annual Revenue, R	$28.33 million
Annual Operating Cost, COM_d	$15.59 million
After-Tax Rate of Return, DCFROR	27.50%
Cost of Capital, i_{coc}	7.0%
NPV at Cost of Capital, CDCF	$58.47 million

Figure S7. *Non-Discounted Cumulative Cash Flow (RXN-ABS, 20 bar)*

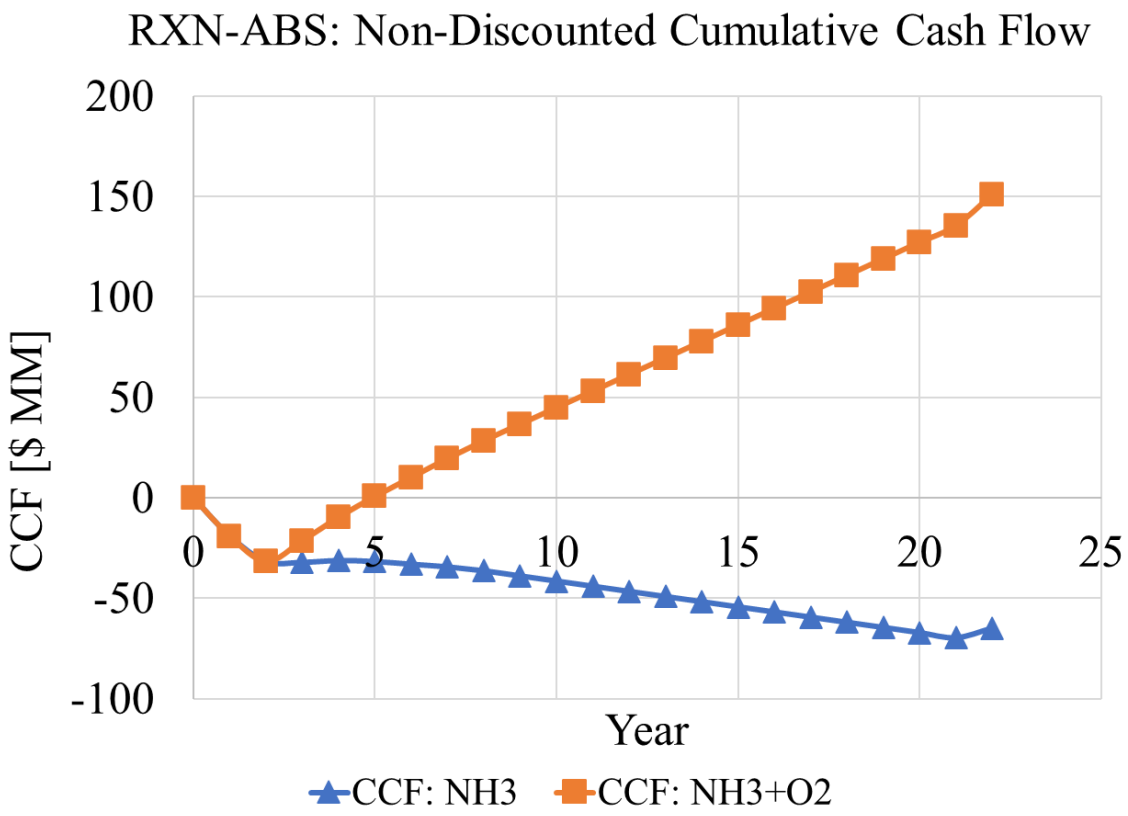

1.12 Cash Flow (RXN-CON) – Selling Oxygen

In Figure S8, non-discounted and discounted cash flow diagram show that the plant can profit after 6 years.

Table S16. *Executive Summary (RXN-CON, 150 bar)*

Executive Summary	
Total Capital Investment, TCI	$34.26 million
Selling Price of Ammonia	$598/MT of ammonia[11]
Annual Revenue: Ammonia	$11.96 million
Annual Revenue: Oxygen	$16.37 million
Total Annual Revenue	$28.33 million
Annual Operating Cost, COM_d	$17.26 million
After-Tax Rate of Return, DCFROR	21.83%
Cost of Capital, i_{coc}	7.0%
NPV at Cost of Capital, CDCF	$46.06 million

Figure S8. *Non-Discounted Cumulative Cash Flow (RXN-CON, 150 bar)*

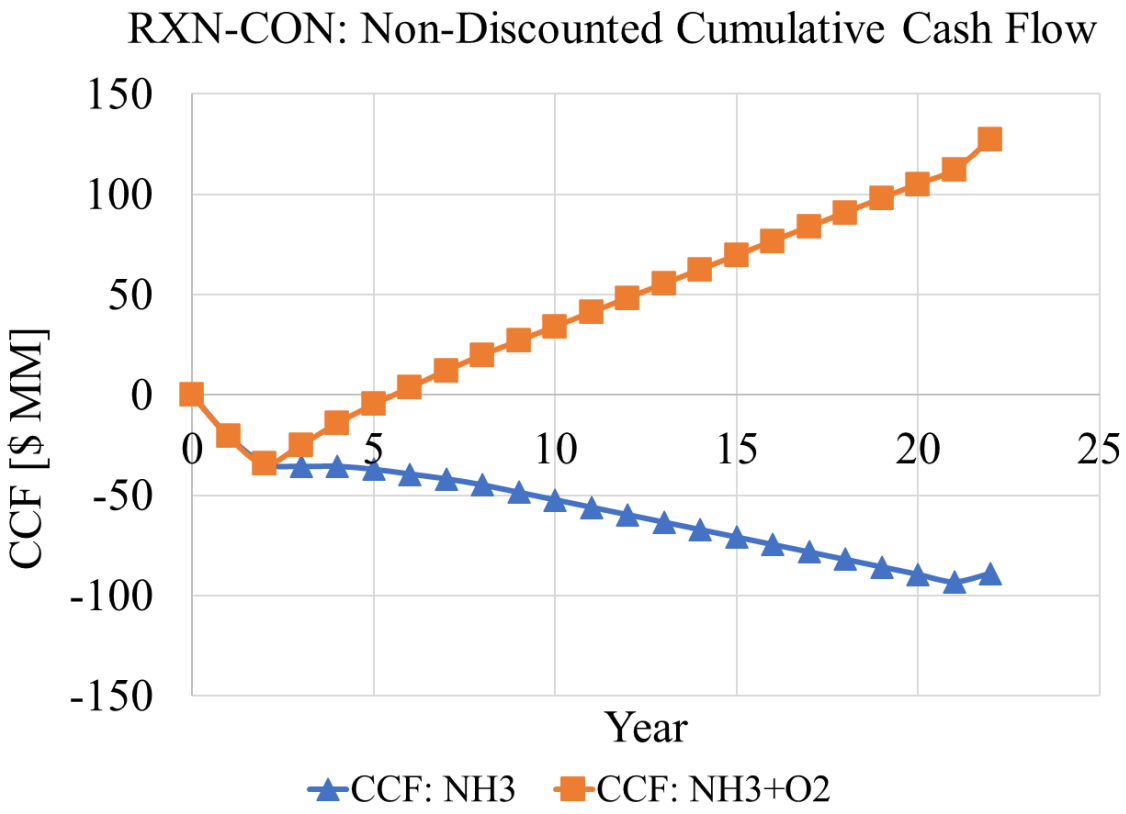

References

(1) Nielsen, A. An Investigation on Promoted Iron Catalysts for the Synthesis of Ammonia; Gjellerup, **1968**; pp 1–264.

(2) Gillespie, L. J.; Beattie, J. A. The Thermodynamic Treatment of Chemical Equilibria in Systems Composed of Real Gases. I. An Approximate Equation for the Mass Action Function Applied to the Existing Data on the Haber Equilibrium. *Phys. Rev.* **1930**, *36* (4), 743–753. DOI: 10.1103/PhysRev.36.743.

(3) Soave, G. Equilibrium Constants from a Modified Redlich-Kwong Equation of State. *Chem. Eng. Sci.* **1972**, *27* (6), 1197–1203. DOI: 10.1016/0009-2509(72)80096-4.

(4) Ruthven, D. M.; Pressure, F. S. K. K. S. Swing Adsorption. In *New York: VCH Publishers*; **1994**; Vol. 1, pp 1–235.

(5) Malmali, M.; Le, G.; Hendrickson, J.; Prince, J.; McCormick, A. V; Cussler, E. L. Better Absorbents for Ammonia Separation. *ACS Sustain. Chem. Eng.* **2018**, *6* (5), 6536–6546. DOI: 10.1021/acssuschemeng.7b04684.

(6) Wei, C.; Sun, Z.; Huang, Y.; Li, L. Embedding Anti-Counterfeiting Features in Metallic Components via Multiple Material Additive Manufacturing. *Addit. Manuf.* **2018**, *24*, 1–12. DOI: 10.1016/j.addma.2018.09.003.

(7) Magnesium bromide (MgBr2). http://periodic-table-of-elements.org/SOLUBILITY/magnesium_bromide (accessed Jul 26, 2020).

(8) Turton, R.; Bailie, R. C.; Whiting, W. B.; Shaeiwitz, J. A. *Analysis, Synthesis and Design of Chemical Processes*; Pearson Education, **2008**.

(9) Galls. Allied Healthcare Products Aluminum O2 Cylinder. https://www.galls.com/allied-healthcare-products-aluminum-d-o2-cylinderWv9zCj-DBoCrFAQAvD_BwE (accessed Jul 28, 2020).

(10) Medical, I. MRI E Cylinder Oxygen Tank. https://www.zzmedical.com/search/mri e cylinder oxygen tank (accessed Jul 28, 2020).

(11) Agricultural Marketing Service - The U.S. Department of Agriculture .

https://www.ers.usda.gov/data-products/fertilizer-use-and-price.aspx (accessed Jan 10, 2020).